scientific reports

Check for updates

OPEN

Study of the effects and mechanism of allogeneic platelet-rich plasma gel on layered skin flaps

Zhengguo Xia[1,9], Feng Han[1,9], Xiaolin Zhan[2], Dongdong Chen[2], Nanyan Luo[2], Wanqi Men[3], Qingyuan Chen[4,9], Junhui Song[4,9], Xinwang Cao[5]✉, YueJun Wang[7], ZhiHao Wang[8], Linsen Fang[1]✉ & Yaohua Yu[6]✉

This study investigated the effects of allogeneic PRP gel on layered flap transplantation in Sprague-Dawley (SD) rats and explored its underlying mechanisms, providing a theoretical foundation for improving clinical layered flap success rates. Seventy-two SD rats were randomly assigned to three groups: layered flap + PRP gel (PRP group), layered flap + saline (control group), and traditional flap + saline (sham group), with 24 rats per group. PRP gel was applied during surgery in the PRP group, while saline was used in the sham and control groups. Skin tissue necrosis, temperature fluctuations, and edema were recorded at 6 h, and on days 1, 3, and 5 post-surgery. Growth factors and inflammatory-related indicators in the skin tissue were analyzed on day 3 post-surgery. Layered skin flap grafts exhibited greater susceptibility to necrosis compared to traditional flaps ($F = 13.754$, $P<0.001$ on 3th day; $F = 10.593$, $P<0.001$ on 5th day). PRP gel enhanced the expression of vascular endothelial growth factor ($F = 9.775$, $P<0.001$), CD31 ($F = 13.181$, $P<0.001$), platelet-derived growth factor ($F = 6.273$, $P<0.001$), and transforming growth factor beta ($F = 8.365$, $P<0.001$), promoting angiogenesis ($F = 17.617$, $P<0.001$). Additionally, PRP reduced the expression of IL-18 ($F = 38.143$, $P<0.001$), IL-1β ($t = 4.575$, $P<0.001$), NLRP3 ($F = 13.016$, $P<0.001$), and caspase-1 ($t = 6.248$, $P<0.001$), thereby mitigating inflammation. These effects contributed to improved layered flap survival rates. Allogeneic PRP gel facilitated neovascularization and reduced inflammation and decreased the necrotic area in the layered skin flap following flap transplantation. The mechanism likely involves the upregulation of local growth factors.

Keywords Platelet-rich plasma gel, Flap survival, NLRP3/caspase-1/IL-β/IL-18 signaling pathway, Growth factors

A complex wound with composite tissue defects involves the loss of two or more types of tissues, necessitating personalized flap designs for effective reconstruction. Improper flap design during repair can lead to postoperative dead space, adversely affecting treatment outcomes[1]. To address these complex wounds, a layered fasciocutaneous flap with a single perforator pedicle was employed. This flap is divided into superficial and deep layers from superficial fat about 2 mm under the superficial fascia: the superficial layer, rich in the subdermal vascular plexus, serves as a skin tissue flap (or subdermal vascular plexus flap) for repairing skin soft tissue defects, while the deep layer, an adipofascial flap, is designed to fill deep cavities. However, the superficial subdermal vascular plexus flap retains only a portion of grade III–IV perforator vessels, making it susceptible to

[1]Department of Reconstructive Surgery and Plastic Surger, The First Affiliated Hospital of Anhui Medical University/Anhui Provincial Public Health Clinical Center, HeFei, China. [2]Department of Ultrasound, The First Affiliated Hospital of Anhui Medical University/Anhui Provincial Public Health Clinical Center, HeFei, China. [3]Department of Clinical Laborator, The First Affiliated Hospital of Anhui Medical University/Anhui Provincial Public Health Clinical Center, HeFei, China. [4]Department of Burns, The First Affiliated Hospital of Anhui Medical University, HeFei, China. [5]Department of Cell Biology, School of Life Sciences, Anhui Medical University, HeFei, China. [6]Department of Burn, Ningbo No.2 Hospital, No. 41 Northwest Street, Haishu District, Ningbo, China. [7]Department of Pathology, Anhui Zhong Ke Geng Jiu Hospital, Hefei, China. [8]Department of Pathology, School of Basic Medical Sciences, Anhui Medical University, Hefei, China. [9]Zhengguo Xia, Feng Han, Qingyuan Chen and Junhui Song contributed equally to this work. ✉email: caoxw@ahmu.edu.cn; shaoshangke@126.com; 529393451@qq.com

distal necrosis and limiting the design ratio of the layered fascial flap. In clinical practice, the maximum initial flap to subdermal vascular plexus flap ratio varies: 1:1 for the trunk and buttocks, 1.71:1 for the thigh, and 2.33:1 for the lower leg[2,3]. Enhancing the stratification ratio of the layered fascial flap to ensure flap survival after transplantation remains a significant challenge in clinical practice.

PRP, a concentrated platelet product derived from blood through centrifugation, was first proposed by Whitman et al. in 1997[4]. Activation is precisely regulated under pulsed electric fields or mechanical fragmentation. PRP's platelets release a variety of growth factors from the a-granules after activation, including PDGF, VEGF, TGF-β, insulin-like growth factor-1, and epidermal growth factor[5]. Studies have demonstrated[6,7] that PRP can enhance flap survival rates by significantly reducing the time required for flap neovascularization, decreasing inflammatory responses, and mitigating ischemia-reperfusion injury. Clinical studies have also demonstrated the effectiveness and safety of using PRP for soft-tissue augmentation by stimulating and enhancing natural repair and regeneration processes[8,9].

Building on these findings, this study utilized a layered flap transplantation model in Sprague-Dawley (SD) rats and applied allogeneic PRP gel during surgery to examine its effects and underlying mechanisms. The aim is to identify novel strategies to enhance the stratification ratio of layered flaps and improve layered flap survival rate.

Experimental animals and materials

Experimental animals

Healthy female Sprague-Dawley (SD) rats ($n = 150$), aged 5 weeks, with body weights ranging from 180 to 220 g, were utilized in this study. Of these, 72 rats were used for the preparation of the experimental model, 72 for blood collection and PRP extraction, and 6 as the normal control group. The experimental animals were purchased from the Experimental Animal Center of Anhui Medical University (License: SYXK [Anhui] 2017-006). This study was approved by the Ethics Committee of Experimental Animals of the Anhui Medical University (approval number: LLSC20221274). All experimental methods were carried out in accordance with relevant guidelines and regulations and are reported in accordance with ARRIVE guidelines. The rats were housed in a controlled environment with a temperature of 20 to 28 °C, humidity ranging from 45% to 75%, and three rats per cage. During the experiment, rats had free access to food and water.

Main reagents and instruments

The following equipment and reagents were used: an -80 °C ultra-low temperature freezer (DW-HL5) (Zhongke Meiling Low Temperature Technology Co., Ltd, Hefei, China), a low-speed desktop centrifuge (L3-5 K) (Kecheng Instrument Equipment Co., Ltd, Hunan, China), ultrasonic diagnostic equipment (ACUSON Sequoia) (Siemens Healthcare Systems Ltd, Munich, Germany), a Ruiwood-enhanced small-animal anesthesia machine (R540) (Ruiwood Biotechnology Co., Ltd, Shenzhen, China), an automated hematology analyzer (BC-5390 CRP) (Mindray International Co., Ltd, Shenzhen, China), an aerosol thermal imaging camera (E3PLUS) (Aeris Electronics Co., Ltd, Shenzhen, China), a high-resolution biological microscope (DP74) (Olympus Co., Ltd., Beijing, China), a real-time PCR instrument (ABI7500) (Thermo Fisher Scientific, Inc., Shanghai, China), and an Odyssey fluorescence imaging system (LICOR Inc., Tucson, USA). Antibodies used included vascular endothelial growth factor (VEGF), transforming growth factor beta (TGF-β), and CD31 antibodies (Maini Biotechnology Development Co., Ltd, Fuzhou, China), platelet-derived growth factor (PDGF) antibody (Zhongshan Golden Bridge Biotechnology Co., Ltd, Beijing, China), and IL-1β, IL-18, caspase-1, and NLRP3 antibodies (Anolun Biotechnology Co., Ltd., Beijing, China). DyLight 800 and goat anti-rabbit antibodies (Anolun Biotechnology Co., Ltd., Beijing, China) were also employed. Other reagents included lyophilized thrombin powder (Leiyusen Pharmaceutical Co., Ltd., Changchun, China) and calcium gluconate (Meida Kanghua Pharmaceutical Co., Ltd., Sichuan, China). Six fluorinated sulfur microbubble injections (Bracco Suisse SA. Geneva, Switzerland).

Experimental methods

PRP grouping and flap model creation

Seventy-eight female SD rats were randomly assigned to four groups: PRP, control, sham, and normal, with 24 rats in each of the PRP, control, and sham groups, and 6 rats in the normal group. Seventy-two female SD rats were used for blood collection to extract PRP gel.

Anesthesia was induced using 3% isoflurane inhalation, and once the rats were fully anesthetized, they were placed in a prone position and secured. Their dorsal fur was shaved and depilated using depilatory cream. A rectangular flap (2 × 6 cm) was designed, with the midline as the medial boundary and the distal end of the scapular angle as the superior boundary. The skin and subcutaneous fascial layers were incised along the marked lines, and the skin tissue layer was separated from the subcutaneous fascia using tissue scissors. During this procedure, the skin tissue layer was maintained with only the thoracodorsal artery perforating vessels, while the fascia layer was preserved with the apical branch of the external carotid artery (Fig. 1). Both the base of the fascia and skin tissue layers were isolated using double layers of gauze soaked in vaseline. In the PRP and control groups, a layered flap model was created. In the sham group, the skin tissue layer was not separated from the subcutaneous fascia, and only a traditional rectangular flap (2 × 6 cm) was formed. PRP gel was applied to the base of both the fascia and skin tissue layers at a concentration of 100 dl/cm^2 in the PRP group, while the control group received an equivalent volume of normal saline. Finally, the fascia and skin tissue layers in both the PRP and control groups were sutured in situ in a layered fashio. In the sham group, 100 dl/cm^2 of normal saline was applied to the base of the flap, and the flap was sutured in situ without further manipulation.

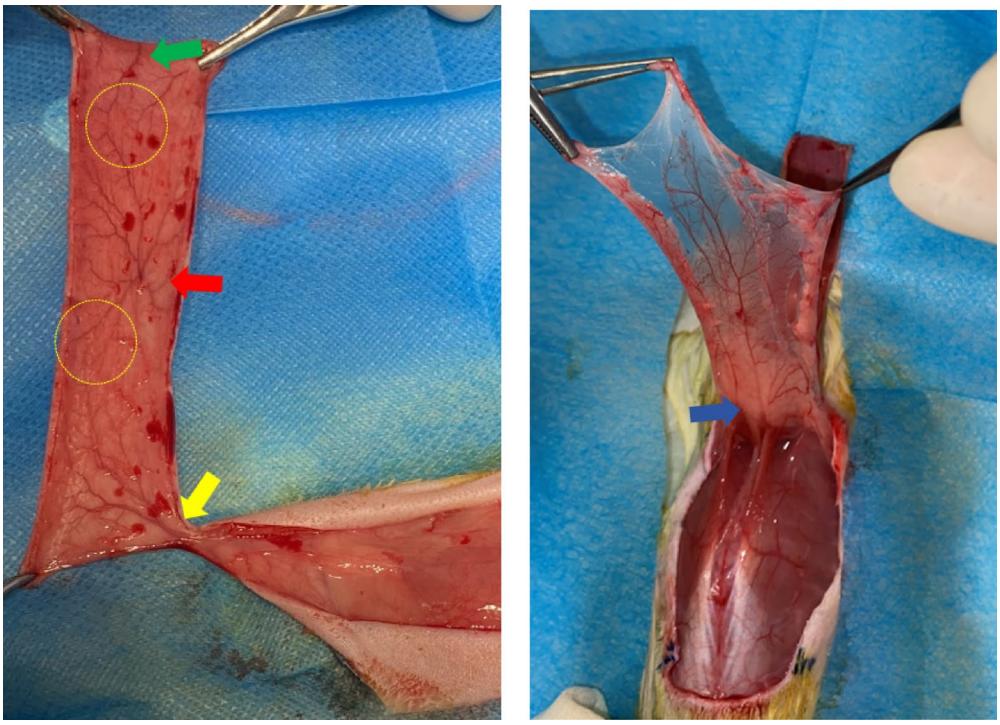

Fig. 1. Schematic diagram of the fabrication of the layered skin flap on the backs. The yellow arrow indicates the perforator vessel of the thoracodorsal artery; the red arrow points to the perforator vessel of the intercostal artery; the green arrow highlights the perforator vessel of the iliolumbar artery; the blue arrow indicates the parietal branch of the external carotid artery. and the yellow circle marks the choke area.

Preparation of allogeneic PRP gel

Before preparing the layered skin flaps for the PRP group, 3 rats were randomly selected from the pool of 72 rats that had undergone blood collection. On average, approximately 2–3 mL of PRP was extracted from every 3 rats, which was then processed into a PRP gel. The detailed steps of the procedure are as follows: Whole blood extraction: The rats were anesthetized with 3% isoflurane inhalation anesthesia, placed in a supine position, secured, disinfected, draped, and an incision was made along the abdominal midline. A 5 mL syringe, pre-lubricated with sodium citrate, was used to puncture the inferior vena cava, and fresh whole blood was drawn into an anticoagulant tube. Euthanizing rats by cervical dislocation under general anesthesia. PRP extraction: PRP was extracted using the Landesberg method[10]. The fresh whole blood was centrifuged at 200 × g (rotor radius, 11 cm) for 20 min. After centrifugation, the plasma and intermediate leukocyte layers were carefully aspirated using a 1 mL syringe and transferred into a new dry tube. This tube was centrifuged again at 200 × g (rotor radius, 11 cm) for an additional 10 min. After centrifugation, the upper half of the plasma was discarded, and the remaining plasma was mixed thoroughly to obtain the PRP. Approximately 0.2 mL of PRP was collected into a sterile EP tube, and a BC-5390 CRP blood cell analyzer was used to count the platelet concentration in the PRP. Preparation of PRP gel: The PRP activator was prepared by mixing 10% calcium gluconate with lyophilized thrombin powder at a concentration of 1,000 U/mL. The PRP was then mixed with the activator in a volume ratio of 10:1 to prepare the PRP gel. All steps were conducted under sterile conditions to avoid contamination of the PRP gel.

Measurement of the skin tissue layer temperature and necrotic area

In the three PRP groups, infrared thermal imaging was used to capture photographs of the skin tissue layers before surgery and on the 6-hour, 1st, 3rd, and 5th days after skin flap transplantation. Concurrently, temperatures at the proximal and distal sites of the skin tissue layer were recorded.

To assess necrosis, the infrared thermal imaging camera was used to capture photographs of the skin tissue layer at the distal end of each group of rats. Necrosis was identified by changes in skin color to black or brown and the skin flap becoming hard and scab-like. Image-Pro Plus software (version 6.0) was employed to analyze the photographs and calculate the necrotic area at the distal end of the skin tissue layer.

Assessing the edema degree of the skin tissue layer

Changes in skin flap thickness in rats can indicate the extent of edema following flap surgery. The thickness of the skin tissue layer at both the proximal and distal ends was measured in the three groups of rats before surgery and at 6 h, 1 day, 3 days, and 5 days post-surgery, using a 10 MHz ultrasound probe.

Central venous catheterization of the common carotid vein and ultrasound angiography

Following flap surgery, the rats were re-anesthetized at 6 h and on the 1st, 3rd, and 5th days post-surgery. After complete anesthesia, the rats were placed in a supine position and secured. The ipsilateral common carotid vein was isolated, and a 24-gauge indwelling needle was inserted into the vein and secured. A 1 mL solution of sulfur hexafluoride microbubbles was then injected *via* the indwelling needle. Ultrasound angiography of the skin tissue layer was performed using a 10 MHz frequency ultrasound probe. The length of the opacification defect at the distal end of the skin tissue layer was recorded for each group.

Platelet count and tissue sampling

At 6 h, and on the 1st, 3rd, and 5th days after flap surgery, tissue samples from the flaps of each group, along with fresh venous blood specimens from the PRP group, were collected. At the center of skin and fascia layers, the tissue specimens were harvested. After fixation with 4% paraformaldehyde, the tissue specimens were stored in a cool, dry place. A blood cell analyzer was used to count the number of platelets in the fresh venous blood from the PRP group, as well as in the corresponding PRP.

Hematoxylin and Eosin (H&E) staining and microvessel counting

Skin tissue layers from each group of rats were embedded in paraffin at various time points post-surgery. Histological sections were prepared and subjected to HE staining. The inflammatory cell count and aggregation within the skin tissue layers were observed at 100x magnification. A comparative analysis of the intensity of the inflammatory response across the different groups was conducted postoperatively. Additionally, on the 3rd day post-surgery, HE-stained sections of the skin tissue layers from each group were examined under 100x magnification. Six discontinuous areas with the highest vascular density were selected, and the number of microvessels was counted. The mean value of these six areas which as the microvascular density for each sample was considered. Microvessels were counted based on the presence of a lumen enclosed by endothelial cells, considered a single, countable microvessel, even if the microvessels originated from the same vessel and meandered within the section.

Real-time RT-PCR

RT-PCR was performed on the skin and fascia layer tissues of the flaps to quantify the relative expression of IL-1β, IL-18, caspase-1, and NLRP3. The skin and fascia layer tissues were homogenized using ultrasonic degradation, and total RNA was extracted using an RNeasy kit. RNA was reverse transcribed into cDNA with a QuantiTect kit. Real-time PCR was conducted using an ABI 7500 QPCR system. The relative expression levels of IL-1β, IL-18, caspase-1, and NLRP3 were quantified using the 2-ΔΔCt method.

Western blot

Western blot (WB) analysis was performed to evaluate the expression levels of IL-1β, IL-18, caspase-1, and NLRP3 in the skin and fascia layers of the flaps on postoperative day 3. Tissue proteins were extracted using a protein extraction kit, followed by electrophoresis and membrane transfer. The membranes were blocked, and primary antibodies were incubated overnight at 4 °C. After primary antibody incubation, an infrared fluorescent secondary antibody was applied and incubated at 25 °C for 2 h. Membranes were scanned using an Odyssey dual-color infrared laser imaging system, and the gray values of target protein bands and internal reference bands were quantified using Image Pro Plus 6.0.

Immunohistochemistry

Paraffin-embedded sections of skin tissue layers tissue from rats were prepared on postoperative day 3, followed by immunohistochemical staining to evaluate the expression of VEGF, TGF-β, CD31 and PDGF. A semi-quantitative scoring method was applied to assess staining intensity. Six randomly selected fields at 400x magnification were scored for each adequately stained slide, with the average of these scores used as the final score. Positivity was defined by the presence of brown or brownish particles localized in the cytoplasm or cell membrane. The percentage of positive cells was calculated relative to the total number of skin tissue cells. The scoring criteria were as follows: (1) Staining intensity: 0 points for no staining, 1 point for pale yellow, 2 points for pale brown, and 3 points for brownish; (2) Percentage of positive cells: 0% scored 0 points, 1%–24% scored 1 point, 25%–49% scored 2 points, 50%–74% scored 3 points, and 75%–100% scored 4 points; (3) The final score was the product of staining intensity and the percentage of positive cells.

Statistical analyses

Data were analyzed using SPSS 24.0. All data conform to a normal distribution, were expressed as the mean ± standard deviation. T-test was used for the comparison between the two groups. One-way analysis of variance (ANOVA) was used for comparisons between groups, with pairwise comparisons conducted using the Bonferroni method. A p-value of < 0.05 was considered statistically significant.

Results

PRP gel affects flap temperature and improves the survival rate of skin flaps

No significant differences were observed in the temperature of the proximal skin tissue layer among the groups prior to surgery ($P > 0.05$). This pattern was consistent postoperatively, with no significant temperature differences at various time points ($P > 0.05$). Over time, a gradual decrease in temperature was observed in the proximal skin tissue layer, but no significant inter-group differences were detected ($P > 0.05$).

Similarly, preoperatively, no significant differences were found in the temperature of the distal skin tissue layer between the groups ($P > 0.05$). Postoperatively, at multiple time points, there were also no significant differences

in distal skin tissue layer temperature between groups ($P > 0.05$). As the postoperative period progressed, the distal skin tissue layer temperature gradually decreased, with no significant differences between groups ($P > 0.05$) (Fig. 2).

At 6 h and on the 1st postoperative day, no necrosis was observed in the distal skin tissue layers of any group. However, by the 3rd postoperative day, necrotic changes were evident in all groups, with the control group showing the most extensive necrosis, significantly different from the sham group ($P < 0.001$). By the 5th postoperative day, the necrotic area in the distal skin tissue layers stabilized across all groups. The control group exhibited a significantly larger necrotic area compared to both the sham and PRP groups, with statistical significance ($P < 0.01$ and $P < 0.05$, respectively) (Fig. 2).

PRP gel delays the peak onset time of flap edema

In the sham group, peak edema in the proximal skin tissue layer occurred on the 3rd postoperative day. In contrast, the PRP group reached peak edema on the 1st postoperative day, significantly different from the sham group ($P < 0.05$). The control group achieved peak edema within 6 h postoperatively, also showing a statistically significant difference compared to the sham group ($P < 0.05$).

For both the sham and PRP groups, peak edema in the distal skin tissue layer occurred on the 3rd postoperative day. However, the control group reached peak edema in the distal skin tissue layer within 6 h postoperatively, with a highly significant difference compared to the sham group ($P < 0.001$).

At all time points, distal edema in the skin tissue layer was more pronounced than proximal edema. However, no statistically significant differences were observed in the thickness of the skin tissue layer between the distal and proximal regions across the groups (Fig. 2).

PRP gel reduces the length of the imaging defect of the flap on ultrasound angiography

Ultrasound contrast defects in the distal skin tissue layers were observed 6 h postoperatively across all groups, with no significant differences between the groups at this time. Over the course of the postoperative period, the length of these contrast defects progressively increased in all groups, stabilizing by the 5th postoperative day. On the 1st, 3rd, and 5th postoperative days, the control group exhibited significantly longer contrast defects than both the sham and PRP groups, with statistically significant differences ($P < 0.05$) (Fig. 2).

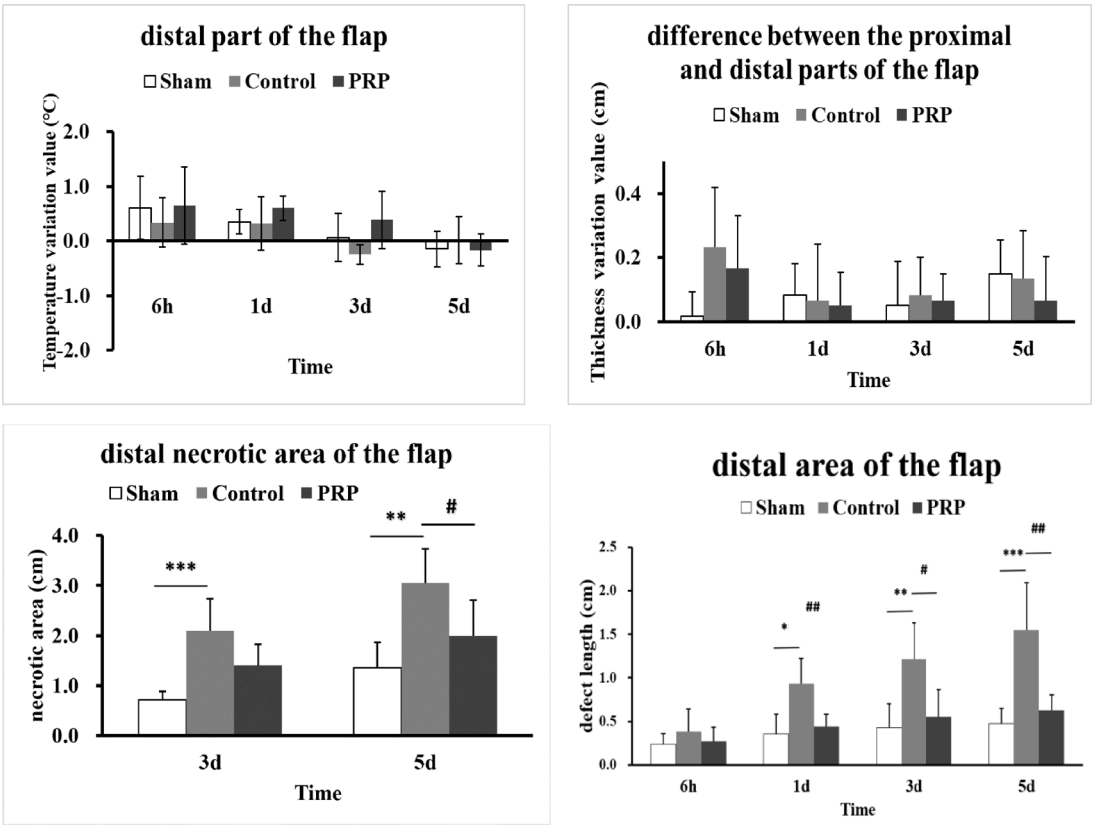

Fig. 2. Comparison of flap distal temperature, edema degree, necrotic area, and defect length under ultrasound contrast at different postoperative time points among different groups. $^{*}P < 0.05$ when comparing the control group with the sham group; $^{**}P < 0.01$; $^{***}P < 0.001$. $^{\#}P < 0.05$ when comparing the PRP group with the control group; $^{\#\#}P < 0.01$.

Number of platelets in the venous blood and applied PRP gel of rats

Platelets, the key components of PRP, were quantified to ensure the optimal concentration of the extracted PRP. The platelet count in the venous blood of the experimental rats was $(632 \pm 93) \times 10^9$/L, while in the PRP, it was $(1703 \pm 247) \times 10^9$/L, indicating that the PRP contained approximately 2.72 times more platelets than the whole blood of the rats.

PRP gel down-regulates inflammation

Inflammatory cell infiltration in the skin tissue layers was first observed 6 h postoperatively in all groups. As the postoperative period progressed, the number of infiltrating inflammatory cells increased, peaking on the 5th postoperative day, with evidence of chronic inflammation. On the 3rd and 5th postoperative days, the PRP (Fig. 3H and J) and sham groups (Fig. 3M and O) showed a significant reduction in inflammatory cell infiltration compared to the control group (Fig. 3C and E).

RT-PCR analysis of inflammatory-related markers in rat skin flap tissues post-surgery indicated that IL-1β and IL-18 expression levels peaked on the 3rd postoperative day, while NLRP3 and caspase-1 levels increased over time (Fig. 4). On the 3rd postoperative day, significant differences in the relative expression levels of IL-1β and IL-18 were observed between the control group and both the sham and PRP groups ($P < 0.001$). By the 5th postoperative day, similar significant differences were noted for IL-1β and NLRP3 between the control and both the sham and PRP groups ($P < 0.001$).

WB for inflammatory-related markers on the 3rd postoperative day corroborated the RT-PCR findings (Fig. 5). The control group exhibited higher expression levels of inflammatory-related markers compared to the PRP and sham groups. Significant differences were observed in cleaved IL-1β, IL-18, NLRP3, and cleaved caspase-1 expression levels between the control and PRP groups ($P < 0.001$).

PRP gel promotes angiogenesis

Neocapillary formation in the skin tissue layer of rats was observed on the 3rd postoperative day across all groups (Fig. 3). On this day, both the PRP and sham groups exhibited a significantly higher number of capillaries (indicated by yellow arrows) compared to the control group, with this difference being statistically significant ($P < 0.05$) (Fig. 3).

PRP gel enhances the expression of growth factors

Immunohistochemical staining for VEGF, PDGF, CD31, and TGF-β on the 3rd postoperative day revealed enhanced expression of these growth factors in the PRP group compared to the control group (Fig. 6). Quantification of the staining intensity in the skin tissue layers showed statistically significant differences between groups ($P < 0.05$) (Fig. 6).

Discussion

PRP can be sourced autologously or allogeneically. Given the limited volume of autologous blood in rats, PRP from allogeneic blood samples was prepared. No significant immune rejection was observed in rats receiving allogeneic PRP, consistent with Akbarzadeh's findings[11]. PRP's platelet concentration is typically 2–5 times higher than that in normal plasma[12]. The optimal platelet dose for promoting angiogenesis in PRP is 1.5×10^{12}/L, as excessively high concentrations may inhibit angiogenesis[13]. The allogeneic PRP obtained had a platelet count of $(1{,}703 \pm 247) \times 10^9$/L, which is 2.72 times higher than normal rat whole blood, indicating an appropriate concentration for the extracted PRP. In previous studies, applying PRP gel at a concentration of 0.1 mL/cm^2 to the flap base[14] has been shown to improve flap perfusion. PRP gel at this concentration was applied to both the skin tissue and fascial flaps to assess its impact on the outcomes of layered flap transplantation.

Infrared thermography serves as a crucial tool for monitoring postoperative temperature variations in flaps and evaluating flap blood perfusion[15,16]. Temperatures were measured at the proximal and distal ends of dorsal skin flaps in three rat groups at multiple pre- and postoperative time points, including temperature differences between the two ends. The results revealed a gradual decrease in temperatures at both ends during the postoperative period; however, no statistically significant differences were observed between the groups. These results differ from those of Han[17], who suggested that postoperative temperature changes exceeding 2.05 °C could indicate necrosis. The observed temperature variations in this study were approximately 1 °C, possibly due to differences in measurement techniques. Temperature measurements were taken from four distinct points at the flap's ends, and as some points did not exhibit necrotic changes, no significant temperature decrease was recorded.

In this study, the control group exhibited a significantly larger necrotic area in the skin tissue layer compared to the PRP group, with peak edema occurring earlier in the control group. The pronounced edema and necrosis in the skin tissue layer of the layered flaps are likely due to the disruption of the vascular network between the skin and subcutaneous fascial layers following flap layering, which impairs blood perfusion and venous return in the skin tissue, making it more prone to edema and necrosis. Application of allogeneic PRP gel delayed the onset of peak edema, mitigating the adverse effects of edema on flap revascularization, enhancing flap blood perfusion, and consequently reducing the necrotic area.

Ultrasound angiography is an effective technique for assessing flap blood perfusion[18,19]. In this study, ultrasound angiography revealed that the PRP group exhibited significantly smaller perfusion defect lengths compared to the control group, suggesting that PRP notably reduced distal filling defects in the flap, consistent with visual assessments of flap necrosis. Compared to visual inspection and infrared thermography, ultrasound angiography provides higher sensitivity and accuracy in predicting and assessing flap necrosis, enabling earlier detection of necrotic changes through flap-filling defects. However, as an invasive procedure, it does not allow for continuous dynamic monitoring. In clinical practice, visual inspection combined with infrared

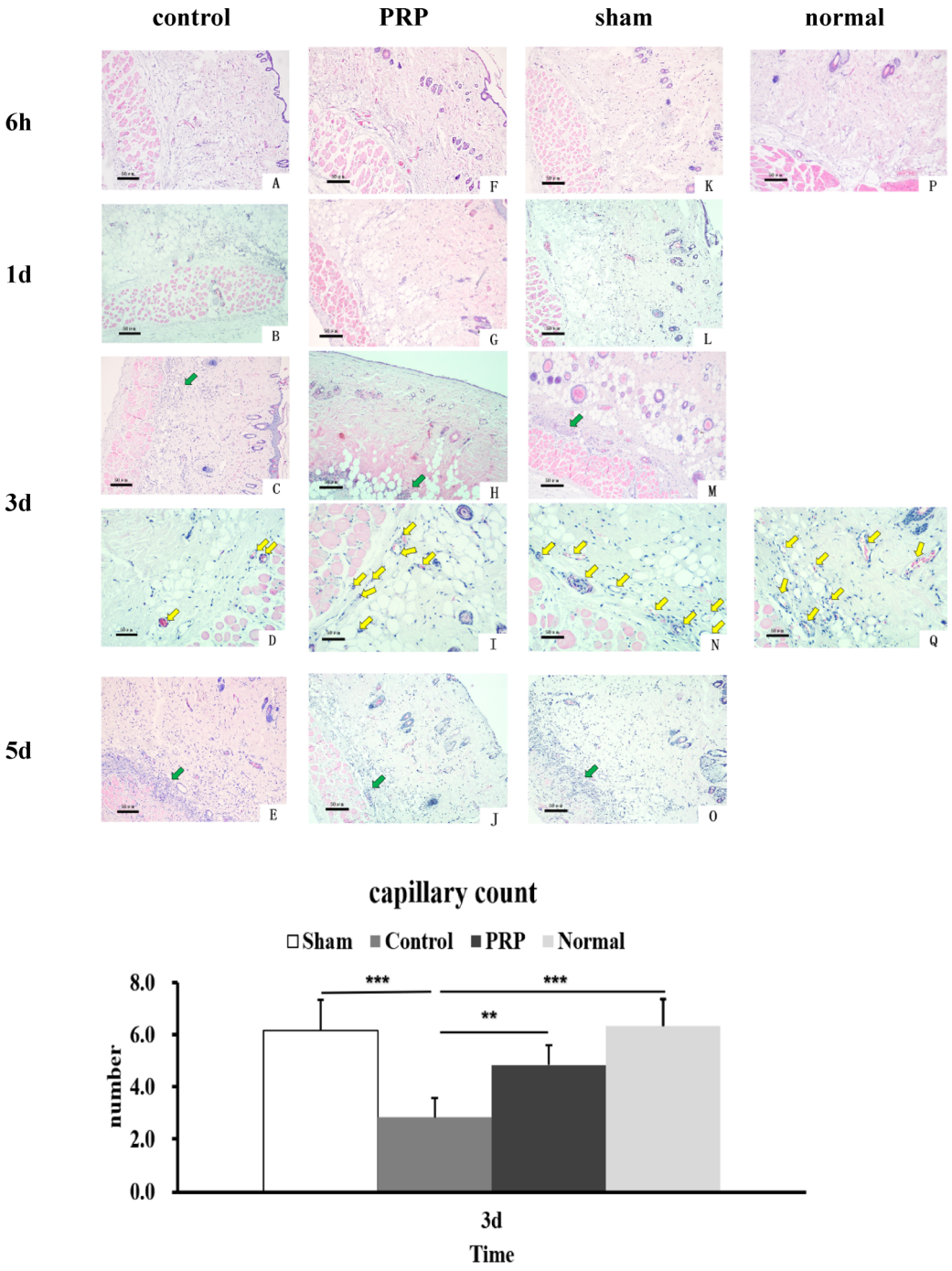

Fig. 3. Schematic diagram of postoperative HE staining results of rat flaps in each group. The green arrow indicates the site of obvious infiltration of inflammatory cells. The yellow arrows indicate the counted microvessels. ** indicates $P < 0.01$, when comparing the control group to the other groups. ***$P < 0.001$.

thermography can be employed for initial dynamic observation of flap perfusion. When these methods are inconclusive, ultrasound angiography should be performed promptly. Timely intervention upon detecting a distal filling defect may prevent or mitigate flap necrosis.

Following flap harvest, disruption of the perforating vessels leads to reduced growth factor activity in flap tissue and a significant decrease in capillary density. A marked reduction in capillaries was observed in the skin tissue layer of fasciocutaneous flaps following layered treatment. HE staining results indicated the formation of new capillaries by the 3rd postoperative day, with the control group exhibiting significantly fewer capillaries than normal tissue and the PRP group, indicating that PRP enhanced capillary formation in the skin tissue layer of the flap. Activated PRP platelets release a variety of growth factors, including VEGF, PDGF, CD31, and TGF-β, which are essential for angiogenesis, local cell proliferation, and infection control. CD31 and VEGF are directly

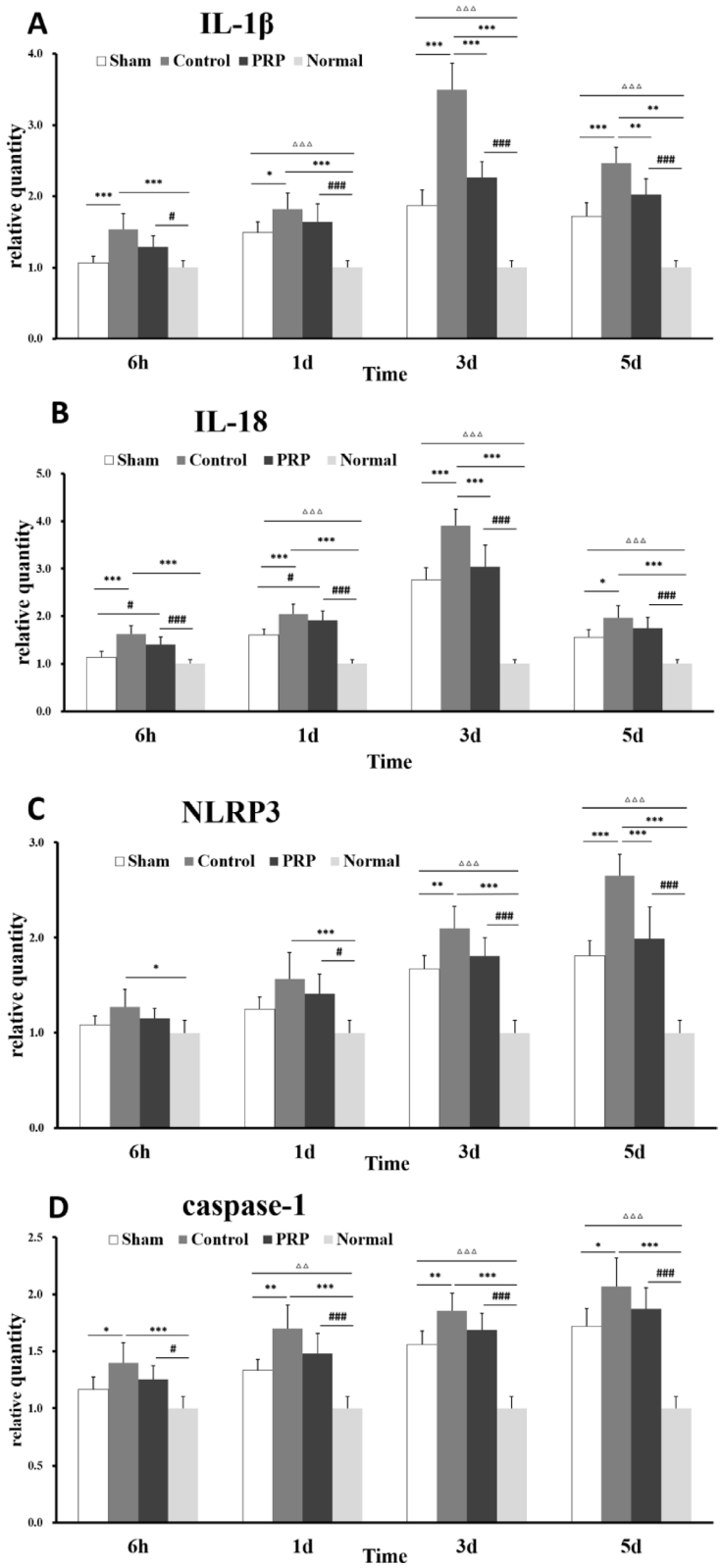

Fig. 4. Statistical chart of q-PCR results from rat skin flap tissues in each group. Note: $^{*}P < 0.05$ when comparing the control group with the other groups; $^{**}P < 0.01$; $^{***}P < 0.001$; $^{\#}P < 0.05$ when comparing the PRP group to the normal and sham groups; $^{\#\#}P < 0.01$; $^{\#\#\#}P < 0.001$; $^{\Delta\Delta\Delta}P < 0.001$ when comparing the sham group to normal tissue; $^{\Delta\Delta}P < 0.01$.

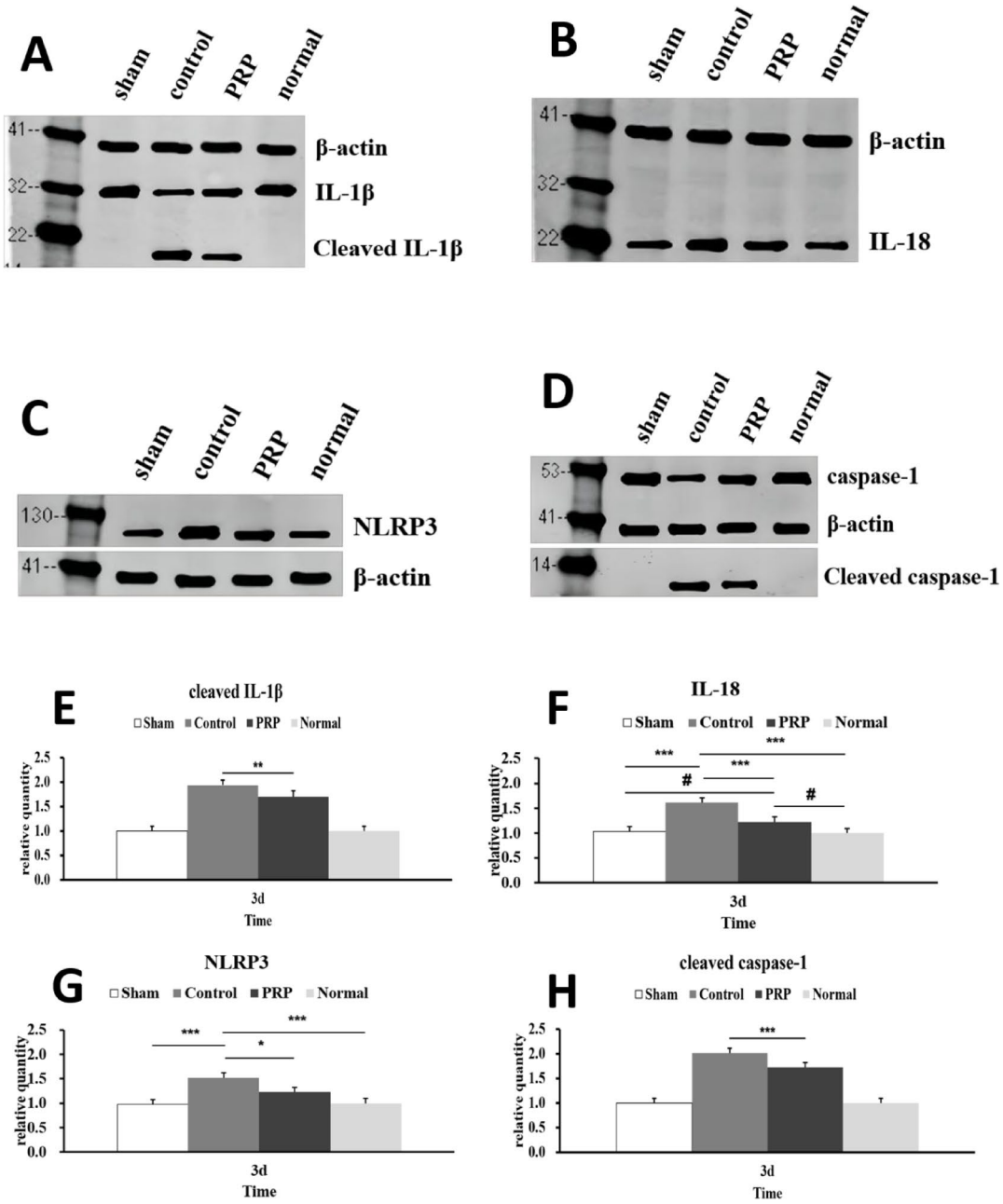

Fig. 5. Western blotting results from rat skin flap tissues on the 3rd postoperative day in each group. Note: $^{*}P<0.05$ when comparing the control group to the other groups; $^{**}P<0.01$; $^{***}P<0.001$; $^{\#}P<0.05$ when comparing the PRP group to the sham group and normal tissue.

involved in new blood vessel formation, while PDGF and TGF-β promote wound healing and tissue repair by enhancing VEGF secretion and stabilizing newly formed blood vessels. Immunohistochemical staining for CD31, VEGF, PDGF, and TGF-β in rat flap skin tissue showed significantly higher expression levels in the PRP group compared to the control group. In summary, PRP may facilitate capillary formation in the skin tissue layer of layered flaps by upregulating VEGF, PDGF, CD31, and TGF-β expression in flap tissue.

NLRP3, caspase-1, IL-1β, and IL-18 are well-established markers of inflammatory responses[20–22]. Caspase-1, a key protease in inflammation regulation, is typically present as an inactive zymogen in the cytoplasm. Upon exposure to pathogens and danger signals, cells assemble inflammasomes, with the NLRP3 inflammasome being the most abundant and structurally complex. This inflammasome recruits pro-caspase-1, which is then activated. Activated caspase-1 cleaves the precursors of IL-1β and IL-18, producing their active forms, which in turn promote the release of mature inflammatory cytokines. IL-1β and IL-18, members of the IL-1 cytokine family, play pivotal roles in modulating inflammatory responses and immune functions[23–25]. Our qPCR analysis revealed that on the 3rd postoperative day, the mRNA expression levels of IL-1β and IL-18 were significantly lower in the PRP group's flap tissue compared to the control group. By the 5th postoperative day, the mRNA

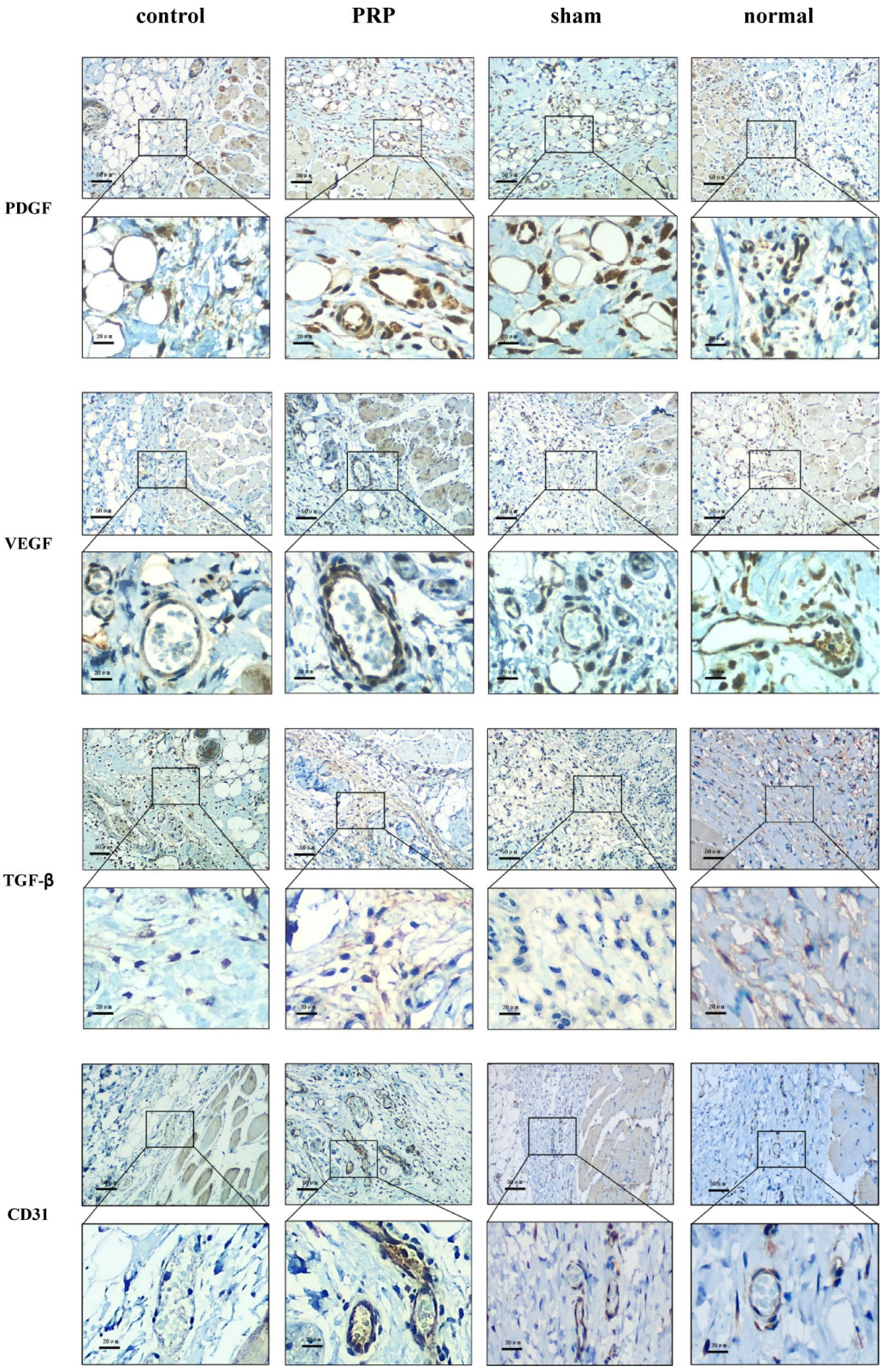

Fig. 6. Immunohistochemistry scores for each group on the 3rd postoperative day. Note: $^{*}P < 0.05$ when comparing the control group to the other groups; $^{**}P < 0.01$; $^{***}P < 0.001$; $^{\#}P < 0.05$ when comparing the PRP group to the normal and sham groups.

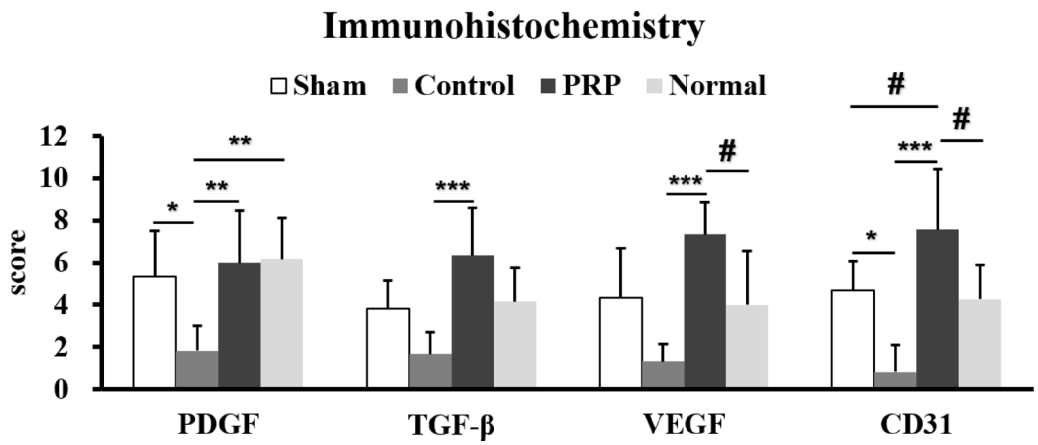

Fig. 6. (continued)

levels of IL-1β and NLRP3 were also notably reduced in the PRP group's flap tissue. WB analysis on the 3rd postoperative day corroborated these findings, showing significantly lower protein expression levels of cleaved IL-1β, IL-18, NLRP3, and cleaved caspase-1 in the PRP group's flap tissue. Furthermore, HE staining on both the 3rd and 5th postoperative days indicated reduced inflammatory cell infiltration and a markedly attenuated inflammatory response in the PRP group's flap tissue relative to the control group. These findings suggest that PRP can mitigate the inflammatory response in flap tissue following layered flap transplantation.

Summary

The application of allogeneic PRP in layered flap transplantation surgery in rats delayed the onset of peak edema in the skin tissue layer, promoted capillary formation in flap tissue, alleviated the inflammatory response and reduced the necrotic area in the skin tissue layer of the flap. The underlying mechanism appears to involve PRP's ability to upregulate the expression of VEGF, CD31, PDGF, and TGF-β while downregulating the expression of IL-1β, IL-18, NLRP3, and caspase-1. This study provides a theoretical foundation for the clinical application of PRP to enhance the success rate of layered flap transplantation.

Data availability

The datasets used and/or analysed during the current study available from the corresponding author on reasonable request.

Received: 16 February 2025; Accepted: 29 September 2025
Published online: 04 November 2025

References

1. Miller, T. J., Lavin, C. V., Momeni, A. & Wan, D. C. Prevention and management of complications of tissue flaps. *Surg. Clin. North. Am.* **101** (5), 813–829 (2021).
2. Xia, Z. et al. Efficacy of treating chronic tibial osteomyelitis with bone defect using a pedicled Perforator-Layered flap and fasciocutaneous flap of the posterior tibial artery: A case report. *Wounds* **32** (11), E50–E54 (2020).
3. Xia, Z. et al. Application of 3 different types of pedicled adipofascial flaps in the repair of deep dead space wounds. *Wounds* **35** (3), 47–52 (2023).
4. Whitman, D. H., Berry, R. L. & Green, D. M. Platelet gel: an autologous alternative to fibrin glue with applications in oral and maxillofacial surgery. *Oral Maxillofac. Surg.* **55** (11), 1294–1299 (1997).
5. Frelinger, A. L. 3rd et al. Tunable activation of therapeutic platelet-rich plasma by pulse electric field: differential effects on clot formation, growth factor release, and platelet morphology. *PLoS One.* **13** (9), e0203557 (2018).
6. Wang, Y., Liu, J., Xie, J., Yu, G. & Luo, Q. The effects of platelet-rich plasma combined with a skin flap transplant on open foot fractures with soft tissue defects. *Am. J. Transl Res.* **13** (6), 6662–6669 (2021).
7. Xie, K. et al. Effect of antilogous Platelet-Rich plasma on the revascularization of rabbit prefabricated flap. *Med. Sci. Monit.* **28**, e937718 (2022).
8. Eppley, B. L., Pietrzak, W. S. & Blanton, M. Platelet-rich plasma: A review of biology and applications in plastic surgery. *Plast. Reconst Surg.* **118** (6), 147e–159e (2006).
9. Eppley, B. L., Woodell, J. E. & Higgins, J. Platelet quantification and growth factor analysis from platelet-rich plasma: implications for wound healing. *Plast. Reconstr. Surg.* **114** (6), 1502–1508 (2004).
10. Xu, J., Gou, L., Zhang, P., Li, H. & Qiu, S. Platelet-rich plasma and regenerative dentistry. *Aust Dent. J.* **65** (2), 131–142 (2020).
11. Akbarzadeh, S., McKenzie, M. B., Rahman, M. M. & Cleland, H. Allogeneic Platelet-Rich plasma: is it safe and effective for wound repair? *Eur. Surg. Res.* **62** (1), 1–9 (2021).
12. Swendseid, B. et al. Platelet-Rich plasma enhances distal flap viability and underlying vascularity in a radiated rotational flap rodent model. *Facial Plast. Surg. Aesthet. Med.* **22** (3), 181–187 (2020).
13. Giusti, I. et al. Identification of an optimal concentration of platelet gel for promoting angiogenesis in human endothelial cells. *Transfusion* **49** (4), 771–778 (2009).
14. Chai, J., Ge, J. & Zou, J. Effect of autologous Platelet-Rich plasma gel on skin flap survival. *Med. Sci. Monit.* **25**, 1611–1620 (2019).
15. Zhang, Y. et al. Infrared thermography-guided designing and harvesting of pre-expanded pedicled flap for head and neck reconstruction. *J. Plast. Reconstr. Aesthet. Surg.* **74** (9), 2068–2075 (2021).

16. Hallock, G. G. Smartphone thermal imaging can enable the safer use of propeller flaps. *Semin Plast. Surg.* **34** (3), 161–164 (2020).
17. Han, T. et al. Indocyanine green angiography predicts tissue necrosis more accurately than thermal imaging and Near-Infrared spectroscopy in a rat perforator flap model. *Plast. Reconstr. Surg.* **146** (5), 1044–1054 (2020).
18. Mueller, S. et al. Contrast-enhanced ultrasonography as a new method for assessing autonomization of pedicled and microvascular free flaps in head and neck reconstructive surgery. *Clin. Hemorheol Microcirc.* **65** (4), 317–325 (2017).
19. Heneweer, C. et al. An innovative approach for preoperative perforator flap planning using Contrast-enhanced B-flow imaging. *Plast. Reconstr. Surg. Glob Open.* **9** (5), e3547 (2021).
20. Li, J. et al. Targeting TFE3 protects against lysosomal Malfunction-Induced pyroptosis in random skin flaps via ROS elimination. *Front. Cell. Dev. Biol.* **9**, 643996 (2021).
21. Xu, J. et al. Platelet-rich plasma attenuates intervertebral disc degeneration via delivering miR-141-3p-containing exosomes. *Cell. Cycle.* **20** (15), 1487–1499 (2021).
22. Chen, L., Wu, D., Zhou, L. & Ye, Y. Platelet-rich plasma promotes diabetic ulcer repair through Inhibition of ferroptosis. *Ann. Transl Med.* **10** (20), 1121 (2022).
23. Sollberger, G., Strittmatter, G. E., Garstkiewicz, M., Sand, J. & Beer, H. D. Caspase-1: the inflammasome and beyond. *Innate Immun.* **20** (2), 115–125 (2014).
24. Kelley, N., Jeltema, D., Duan, Y. & He, Y. The NLRP3 inflammasome: an overview of mechanisms of activation and regulation. *Int. J. Mol. Sci.* **20** (13), 3328 (2019).
25. Martin, P., Goldstein, J. D., Mermoud, L., Diaz-Barreiro, A. & Palmer, G. IL-1 family antagonists in mouse and human skin inflammation. *Front. Immunol.* **12**, 652846 (2021).

Acknowledgements

This study was supported by Anhui Medical University Clinical Medicine Peak Discipline Construction Project (9301001810, 9301001815), Anhui Medical University First Affiliated Hospital North District Research Cultivation Fund Project (2021YKJ012), Anhui Medical University Clinical Science Fund Project (2019xkj156). We also extend our gratitude to Anhui Medical University for their consultation and provision of instruments that facilitated this work.

Author contributions

Conception and Study design: ZGX, LSF, FHLiterature Review: ZGX, QYC, FHData acquisition: XLZ, DDC, NYL, ZHW, YJW, WQMData Analysis and Interpretation: ZGX, FH, LSF, YHY, QYC Drafting of the manuscript: LSF, ZGX, JYS, YHYCritical revision: JYS, ZGX, FH, XWC.

Declarations

Competing interests

The authors declare no competing interests.

Additional information

Supplementary Information The online version contains supplementary material available at https://doi.org/10.1038/s41598-025-22405-4.

Correspondence and requests for materials should be addressed to X.C., L.F. or Y.Y.